

Published in final edited form as:

Nucl Med Biol. 2013 August ; 40(6): 788–794. doi:10.1016/j.nucmedbio.2013.04.006.

Specific uptake of ^{99m}Tc -NC100692, an $\alpha_v\beta_3$ -targeted imaging probe, in subcutaneous and orthotopic tumors[★]

Jason L.J. Dearling^{a,b,*}, Jessica W. Barnes^{b,c,d,e}, Dipak Panigrahy^{b,c,d,e}, Robert E. Zimmerman^{b,f}, Frederic Fahey^{a,b}, S.Ted Treves^{a,b}, Matthew S. Morrison^g, Mark W. Kieran^{b,c,d,e}, and Alan B. Packard^{a,b}

^aDivision of Nuclear Medicine and Molecular Imaging, Department of Radiology, Boston Children's Hospital, Boston, TX, USA

^bHarvard Medical School, Boston, TX, USA

^cVascular Biology Program, Boston Children's Hospital, Boston, TX, USA

^dDivision of Pediatric Oncology, Dana-Farber Cancer Institute, United Kingdom

^eHematology/Oncology, Dana-Farber Children's Hospital Cancer Center, United Kingdom

^fDepartment of Radiology, Brigham and Women's Hospital, United Kingdom

^gGE Healthcare, Medical Diagnostics, The Grove Centre, Amersham HP7 9LL, United Kingdom

Abstract

Introduction—The $\alpha_v\beta_3$ integrin, which is expressed by angiogenic epithelium and some tumor cells, is an attractive target for the development of both imaging agents and therapeutics. While optimal implementation of $\alpha_v\beta_3$ -targeted therapeutics will require a priori identification of the presence of the target, the clinical evaluation of these compounds has typically not included parallel studies with $\alpha_v\beta_3$ -targeted diagnostics. This is at least partly due to the relatively limited availability of PET radiopharmaceuticals in comparison to those labeled with ^{99m}Tc . In an effort to begin to address this limitation, we evaluated the tumor uptake of ^{99m}Tc -NC100692, a cyclic RGD peptide that binds to $\alpha_v\beta_3$ with ~ 1 -nM affinity in an $\alpha_v\beta_3$ -positive tumor model as well as its in vivo specificity.

Methods—MicroSPECT imaging was used to assess the ability of cilengitide, a therapeutic with high affinity for $\alpha_v\beta_3$, to block and displace ^{99m}Tc -NC100692 in an orthotopic U87 glioma tumor. The specificity of ^{99m}Tc -NC100692 was quantitatively evaluated in mice bearing subcutaneous U87MG tumors, by comparison of the biodistribution of ^{99m}Tc -NC100692 with that of the non-specific structural analogue ^{99m}Tc -AH-111744 and by blocking uptake of ^{99m}Tc -NC100692 with excess unlabeled NC100692.

[★]The authors declare that they have no conflict of interest.

© 2013 Published by Elsevier Inc.

^{*}Corresponding author. Division of Nuclear Medicine and Molecular Imaging, Department of Radiology, Boston Children's Hospital, Boston, MA 02115, USA. Tel.: +1-617-9192106; fax: +1-617-7300619. jason.dearling@childrens.harvard.edu (Jason L.J. Dearling).

Supplementary data to this article can be found online at <http://dx.doi.org/10.1016/j.nucmedbio.2013.04.006>.

Results—MicroSPECT imaging studies demonstrated that uptake of ^{99m}Tc -NC100692 in the intracranial tumor model was both blocked and displaced by the $\alpha_v\beta_3$ -targeted therapeutic cilengitide. Biodistribution studies provided quantitative confirmation of these imaging results. Tumor uptake of ^{99m}Tc -NC100692 at 1 h post-injection was $2.8 \pm 0.7\%$ ID/g compared to $0.38 \pm 0.1\%$ ID/g for ^{99m}Tc -AH-111744 ($p < 0.001$). Blocking ^{99m}Tc -NC100692 uptake by pre-injecting the mice with excess unlabeled NC100692 reduced tumor uptake by approximately fivefold, to $0.68 \pm 0.3\%$ ID/g ($p = 0.01$).

Conclusion—These results confirm that ^{99m}Tc -NC100692 does, in fact, target the $\alpha_v\beta_3$ and may, therefore, be useful in identifying patients prior to anti- $\alpha_v\beta_3$ therapy as well as monitoring the response of these patients to therapy.

Keywords

Angiogenesis; NC100692; MicroSPECT; $\alpha_v\beta_3$; Brain tumor; RGD peptides; Cilengitide

1. Introduction

Angiogenesis, the formation of blood vessels from existing host vasculature, is one of the principal ways by which tumors become vascularized. Antiangiogenic therapies thus offer an attractive therapeutic mechanism for cancer in which the blood flow to the lesion(s) is disrupted, starving the constituent tumor cells [1]. However, for this therapy to be successful it is necessary that the therapeutic target be present on the cancer cells. Molecular imaging, using probes targeted to the same receptors as the therapeutics, has the potential to identify that subset of patients that are most likely to respond to a specific therapy.

The integrin $\alpha_v\beta_3$ is known to be expressed at high levels in angiogenic regions of tumors and is also known to be involved in the angiogenic process [2]. Therapeutic agents have been developed that include the arginine–glycine–aspartic acid (RGD) peptide sequence, which binds to the $\alpha_v\beta_3$ (vitronectin) receptor and interferes with its function, slowing tumor growth. These agents include the cyclic pentapeptide cilengitide (Merck KGaA EMD121974) (Fig. 1B). The use of molecular imaging probes to characterize $\alpha_v\beta_3$ expression in tumors therefore offers the potential to improve the clinical success of this therapy by identifying those patients who are most likely to respond to anti- $\alpha_v\beta_3$ therapeutics.

A number of PET and SPECT probes that incorporate the RGD sequence have been developed for evaluating $\alpha_v\beta_3$ expression. The first example was by Haubner et al. [3] who reported the ^{125}I labeling and biodistribution of c(RGDyV) and c(RGDfY) in mice bearing M21, MACaF, and induced osteosarcoma tumors and observed that the ^{125}I -labeled c(RGDyV) peptide had high affinity and selectivity for the $\alpha_v\beta_3$ integrin. Other radiolabeled RGD peptides have since been reported including ^{99m}Tc , ^{18}F , ^{64}Cu and ^{68}Ga -labeled agents [4,5]. As NC100692 is labeled with the widely used radionuclide ^{99m}Tc , with its ideal emissions for clinical imaging, it has potential for more wide-spread application than other less available radionuclides. Studies have reported the use of ^{99m}Tc -NC100692 both in the preclinical detection of angiogenesis following myocardial infarction or ischemia and in the clinical detection of tumors [6–10]. However, its biodistribution and specificity of tumor

targeting in tumor-bearing animals were not previously reported. In this study, we address this deficiency by reporting the biodistribution and tumor localization of ^{99m}Tc -NC100692 in a murine model of glioma including evaluation of its target specificity.

Molecular imaging using radiolabeled probes has the potential to confirm the presence of a biological target and also to monitor therapeutic progress through quantitative characterization of the tumor cell in vivo. Here, we investigate the specificity of tumor localization of ^{99m}Tc -NC100692 (Fig. 1A) [11], an imaging probe for the detection of expression of the integrin $\alpha\text{v}\beta 3$ by tumor cells and angiogenic endothelium.

2. Materials and methods

2.1. General

NC100692 (maraciclatide) was supplied by GE Healthcare (Amersham, UK). EMD121974 (cilengitide) was supplied by Merck KGaA (Darmstadt, Germany). All other chemicals and reagents were of standard reagent grade and were used as received. The ^{99m}Tc concentration in tissue samples was assayed using a Packard Cobra gamma counter (Perkin-Elmer, Waltham, MA).

2.2. Animal model

All animal studies were carried out under protocols reviewed and approved by the Institutional Animal Care and Use Committees (Boston Children's Hospital and Harvard Medical School).

2.3. ^{99m}Tc -NC100692 preparation

Technetium-99m labeling of NC100692 and quality control procedures were carried out according to the manufacturer's instructions. Briefly, the lyophilized kit was reconstituted with 6.0 mL of sodium pertechnetate ^{99m}Tc with a radioactive concentration between 0.206 and 0.223 GBq/mL and incubated at room temperature for 15 min. The labeling efficiency was measured by TLC using ITLC-SG strips (Pall Life Sciences, Ann Arbor, MI) and methanol/1 M ammonium acetate (1:3 vol/vol) as the mobile phase. Using these conditions, ^{99m}Tc -NC100692 has an RF of 0.33 while $^{99m}\text{TcO}_4^-$ ("free pertechnetate") moves at the solvent front and "reduced hydrolyzed technetium" remains at the origin (see Supplementary Figure 1). The manufacturer's instructions require that > 85% of the activity be between RF = 0.07 and 0.54 for clinical use. The radiochemical purity of the final product was greater than 95% for these studies.

2.4. Biodistribution studies

Biodistribution studies were carried out using a subcutaneous glioblastoma (U87MG) tumor model stably transfected with luciferase, and were a gift from Dr. Andrew Kung of the Dana-Farber Cancer Institute, Boston. The tumors were induced by subcutaneous injection of 1×10^6 cells. The tumors were allowed to grow until they were approximately 0.5 cm in diameter. Tumor growth was monitored using their luciferase expression. Briefly, mice were anesthetized, injected with D-luciferin at 50 mg/mL i.p. (Xenogen, Alameda, CA), and imaged with the IVIS 200 Imaging System (Xenogen) for 10–120 s, bin size 2.

For the biodistribution study, each animal was injected with 740 kBq (20 μ Ci) of ^{99m}Tc -NC100692 (typically containing 0.083 μg of peptide) in 100 μL of saline via the lateral tail vein. At each time point post-injection (p.i.) (15, 30, 60, 120 min.), animals ($n = 4-6$) were sacrificed (CO_2 asphyxia) and selected organs excised, weighed, and assayed for ^{99m}Tc . The percentage injected dose (%ID/g) in each tissue was calculated by comparison of the tissue counts to standard samples prepared from the injectate.

To investigate the specificity of organ uptake, a non-specific structural analogue of NC100692 with its RGD pharmacophore scrambled to DRG (designated AH-111744) was radiolabeled with ^{99m}Tc and its biodistribution at 60 min p.i. measured.

The effect of pre-injection of excess mass (2000 \times) of unlabeled NC100692 on the biodistribution of the radiotracer was also investigated.¹ NC100692 in saline (165 μg in 200 μL) was injected intraperitoneally (i.p.), followed 30 min later by injection of the labeled tracer as described above. Thirty minutes after injection of ^{99m}Tc -NC100692 the mice were sacrificed, and the biodistribution of the ^{99m}Tc was assayed.

2.5. MicroSPECT imaging

Imaging studies were carried out using both subcutaneously implanted U87MG and HeLa cells, and separately, orthotopically implanted U87MG tumor cells as an intracerebral model of glioma. Subcutaneous tumor models were created as described above. HeLa cells were implanted on the contralateral flank as target negative controls (for relative expression of $\alpha_v\beta_3$ by these two cell lines, see Ref. [12]). For the orthotopic tumor model, mice were anesthetized by isoflurane and received a stereotactically guided injection of 1×10^5 human U87MG glioblastoma cells into the forebrain (2 mm lateral and 1 mm anterior to the bregma).

MicroSPECT imaging was performed using the Harvard Medical School microSPECT imaging system [13,14]. Briefly, this system consists of a large field of view triple-headed gamma camera with six pinholes, two per detector. For these studies, 0.8-mm pinhole apertures were used resulting in a system spatial resolution for ^{99m}Tc of 0.8 mm.

Prior to imaging, each animal was injected with 37 MBq (1 mCi) of ^{99m}Tc -NC100692 in 100 μL saline via the lateral tail vein while the animals were under isoflurane anesthesia (1%–2% in oxygen), and anesthesia was maintained throughout the data collection period. Immediately after injection, the mice were placed in the imaging tube and a dynamic microSPECT acquisition was begun; 12 rotations of 5 min each for a total imaging time of 60 min were performed. Images were reconstructed using OSEM reconstruction for each of the 12 rotations. Using ImageJ, ROIs were defined on the resulting images for the tumor, normal brain region and local non-target soft tissue. Time–activity curves were then derived from these ROIs.

The ability of cilengitide to displace the tumor uptake of ^{99m}Tc -NC100692 was also evaluated using microSPECT imaging. Cilengitide in saline (50 mg/kg, 1.25 mg for a 25 g

¹These studies were carried out with the unlabeled peptide because cilengitide was not available due to regulatory issues.

mouse, molar excess of approximately 44,000 ×) was injected i.p. into tumor-bearing mice 30 min after injection of $^{99m}\text{Tc-NC100692}$.

2.6. Small-animal MRI studies

MRI studies were carried out at the Harvard Medical School's NeuroDiscovery Center using a 33-cm-wide-bore Oxford 4.7-T magnet with a Bruker Biospec Avance console running XWINNMR and Paravision 3.02 software, including the Bruker diffusion package and a ^1H surface coil optimized for imaging the mouse brain. Contrast-enhanced studies were carried out after intraperitoneal injection of Gd-DTPA (Magnevist, Berlex, Montville, NJ).

2.7. Image fusion

Automatic image registration was performed using a Hermes workstation (Hermes Medical Solutions, Stockholm, Sweden).

2.8. Statistical analysis

Biodistribution data are reported as the mean of four to six mice per data point ± 1 standard deviation (SD). Statistical analysis was carried out using SPSS v19. Student's *t*-test was used to compare data (independent samples, equal variances assumed) with differences considered statistically significant at the 5% level ($p < 0.05$). Outlying data points were rejected according to Chauvenet's criterion [15].

3. Results

3.1. Biodistribution

The results of the biodistribution studies are shown in Fig. 2. The data in Fig. 2A show that the tumor uptake increased from 15 min ($1.95 \pm 0.31\%$ ID/g, mean \pm standard deviation) to peak at 30–60 min (2.59 ± 0.99 and $2.81 \pm 0.74\%$ ID/g, respectively), and then decreased by 120 min ($1.01 \pm 0.09\%$ ID/g). Kidney and gut uptake were highest at 15 min p.i. (4.73 ± 0.83 , $4.98 \pm 1.17\%$ ID/g, respectively), decreasing to approximately 2% ID/g by 120 min p.i. (2.27 ± 1.05 and $1.82 \pm 0.76\%$ ID/g, respectively).

The target specificity was evaluated by comparing the biodistribution of a non-specific structural analogue of NC100692 in which the RGD pharmacophore was scrambled to DRG (designated AH-111744) to that of $^{99m}\text{Tc-NC100692}$. The tumor uptake of the non-specific peptide at 60 min p.i. (Fig. 2B) was much lower than that of NC100692; only $0.37 \pm 0.12\%$ ID/g compared with $2.81 \pm 0.74\%$ ID/g ($p < 0.001$). Uptake of the non-specific agent was also lower than $^{99m}\text{Tc-NC100692}$ in all other tissues ($p < 0.035$) except blood ($p = 0.072$).

The ability of excess unlabeled NC100692 (2000-fold excess by mass) to block the uptake of the ^{99m}Tc -labeled agent was also investigated. The data in Fig. 2C indicate that the tumor uptake of $^{99m}\text{Tc-NC100692}$ was decreased by almost fivefold in the blocked group compared with saline injected controls (saline control $3.15 \pm 1.58\%$ ID/g; blocked $0.68 \pm 0.31\%$ ID/g; $p < 0.011$). As with the biodistribution of the non-specific peptide, blocking significantly decreased $^{99m}\text{Tc-NC100692}$ uptake in all other tissues ($p < 0.043$) except blood ($p = 0.49$).

3.2. MicroSPECT imaging

In vivo microSPECT imaging was also used to evaluate the biodistribution and tumor uptake of ^{99m}Tc -NC100692 in the subcutaneous glioma model. Fig. 3 shows the results of an imaging study in which the localization of ^{99m}Tc -NC100692 in $\alpha_v\beta_3$ -positive U87MG tumors was compared with the uptake in $\alpha_v\beta_3$ -negative HeLa tumors. Fig. 3 shows the location of the U87MG tumor using Xenogen imaging. Fig. 3B shows that the uptake of ^{99m}Tc -NC100692 in U87MG tumors is much higher than in the HeLa tumors. Fig. 3C shows the decrease in uptake following injection of cilengitide (intraperitoneal injection, 50 mg/kg) 30 min after injection of ^{99m}Tc -NC100692. Technetium-99m-NC100692 is displaced from the tumor by cilengitide, confirming the common in vivo target of these agents. Fig. 3D shows the time-activity curve for the tumor uptake of ^{99m}Tc -NC100692 in the U87MG subcutaneous tumor over 60 min and its displacement by cilengitide.

Fig. 4 shows the results of a microSPECT imaging study in which the localization of ^{99m}Tc -NC100692 in orthotopic intracranial tumors was investigated. Both the images (Fig. 4A–C) and the time-activity curves (Fig. 4D) support the observation that ^{99m}Tc -NC100692 uptake in the orthotopic tumor is higher than in normal brain or local soft tissue. In a separate imaging study (Fig. 5), two anomalies were detected by MRI (Fig. 5A, regions 1 and 2), but only one was positive for ^{99m}Tc -NC100692 uptake in subsequent microSPECT imaging (Fig. 5B). Histopathological analysis (Figs. 5D, E) revealed that region 1 was hemorrhage and therefore $\alpha_v\beta_3$ negative and that region 2 contained tumor cells, emphasizing the specificity of the tracer.

4. Discussion

In this study the biodistribution and specificity of target uptake of the $\alpha_v\beta_3$ -targeted radiolabeled peptide ^{99m}Tc -NC100692 were measured in mice bearing subcutaneous and orthotopic $\alpha_v\beta_3$ -positive glioma tumors. Tumor uptake peaked at approximately 1 h and was specific for the $\alpha_v\beta_3$ target, as shown by both blocking and displacement studies. MicroSPECT imaging studies in mice bearing subcutaneous U87MG ($\alpha_v\beta_3$ -positive) tumors and contralateral HeLa ($\alpha_v\beta_3$ -negative) tumors showed that uptake of the agent was higher in the U87MG tumors and that uptake of ^{99m}Tc -NC100692 in the U87MG tumors was decreased by cilengitide, a therapeutic agent that also targets the $\alpha_v\beta_3$ receptor.

The agent rapidly cleared from normal tissues with some retention in the kidneys and intestines that may be receptor mediated. Specific uptake in the gut has been reported for other RGD peptides (e.g. Refs. [16,17]), and the lower gut uptake in the studies with the non- $\alpha_v\beta_3$ -specific DRG peptide suggests that this uptake is receptor mediated for NC100692. Specific uptake of ^{99m}Tc -NC100692 by normal tissues is also suggested by observation that, as has been described by previous studies (e.g. Ref. [18]), injection of excess mass of unlabeled peptide (2000-fold) decreases uptake in these tissues.

Technetium-NC100692 has been used to detect cancer in at least two clinical studies. Bach-Gansmo et al. [8,9] reported the results of SPECT imaging with ^{99m}Tc -NC100692 in 27 patients. Breast cancer lesions were successfully detected in all 27 patients, but not all known lesions were identified. The discrepancy may be due to the absence of $\alpha_v\beta_3$ expression in the

lesions that were not detected, but no histological studies were carried out so this cannot be confirmed. In another clinical study, Axelsson et al. [10] used ^{99m}Tc -NC100692 to detect metastases from breast and lung cancers. They found that some metastases, especially to the lung and brain, were detected, but there were differences between the numbers of lesions detected with SPECT and reference imaging (CT and MRI). However, as with the report by Bach-Gansmo et al. [8,9], there was no histological confirmation of $\alpha_v\beta_3$ expression in the lesions. In combination, these two studies reinforce the concept that the results of imaging studies performed with receptor-targeted radio-pharmaceuticals such as ^{99m}Tc -NC100692 must be interpreted with caution, since the absence of tracer uptake by a lesion may not reflect a lack of sensitivity but rather the lack of expression of the receptor by that lesion.

Technetium-99m-NC100692 is one of several ^{99m}Tc -labeled peptides that have been developed to image $\alpha_v\beta_3$ expression. These compounds vary in their choice of chelator, the linker between the chelator and the peptide, and the peptide itself. For example, Kunstler et al. [19] reported that, in a series of three ^{99m}Tc “4 + 1” mixed-ligand RGD derivatives, decreased chelator lipophilicity was associated with decreased hepatobiliary excretion and increased urinary excretion. Decristoforo et al. [20] made a similar observation when they compared four different Tc-cores, including ^{99m}Tc -EDDA/HYNIC-peptide (where EDDA is ethylenediamine *N,N'*-diacetic acid, and HYNIC is hydrazinonicotinamide) which had the most favorable pharmacokinetics, including low intestinal excretion and rapid renal clearance. Liu et al. [21], also investigating the ^{99m}Tc -HYNIC core, found that the co-ligand charge had a significant effect on peptide clearance. Use of ISONIC and PDA (isonicotinic acid and 2,5-pyridinedicarboxylic acid, respectively) as co-ligands resulted in improved kidney clearance compared with the more highly charged TPPTS (trisodium triphenylphosphine-3,3',3''-trisulfonate), with kidney uptakes of 6.11 (ISONIC), 8.44 (PDA) and 14.33% ID/g (TPPTS) at 120 min p.i.

For ^{99m}Tc -NC100692, introducing a PEG (polyethylene glycol) moiety into the structure (Fig. 1A) extended the blood half-life, increasing absolute tumor uptake [11]. Liu et al. [16] observed a similar effect. Incorporation of a triglycine (G3) and two PEG4 linkers into an RGD peptide increased both in vitro target affinity and in vivo tumor uptake compared with the control molecule (from approximately 2% ID/g for the control to approximately 6% ID/g for the G3PEG4 dimer).

Tumor uptake can also be increased by increasing the number of RGD units included in the tracer. Lui et al. [17] compared a tetramer and a dimer derivative and found that the tetramer showed improved tumor uptake compared with the dimer (~3% ID/g for the dimer vs. ~6% ID/g for the tetramer at 60 min p.i.) as well as more rapid clearance from the blood, intestine, and liver. However, this improvement was offset by the relatively high kidney uptake of the tetramer (26% ID/g at 120 min p.i.) compared with the dimer (15% ID/g at 120 min p.i.). In comparison, ^{99m}Tc -NC100692 has lower uptake in the kidney (<6% ID/g at all time points, Fig. 2) while retaining high tumor uptake (3% ID/g at 60 min p.i.).

5. Conclusions

In this study, the ^{99m}Tc -labeled peptide NC100692 was shown to specifically target the $\alpha_v\beta_3$ receptor and to have good pharmacokinetic properties with respect to clearance from non-target tissues. In microSPECT imaging studies ^{99m}Tc -NC100692 was shown to share a biological target with the anti-angiogenic therapeutic agent cilengitide. It thus has the potential to be used as an imaging agent to guide the selection of patients with tumors that express the $\alpha_v\beta_3$ receptor and are, therefore most likely to respond to anti- $\alpha_v\beta_3$ therapeutics, such as cilengitide.

Supplementary Material

Refer to Web version on PubMed Central for supplementary material.

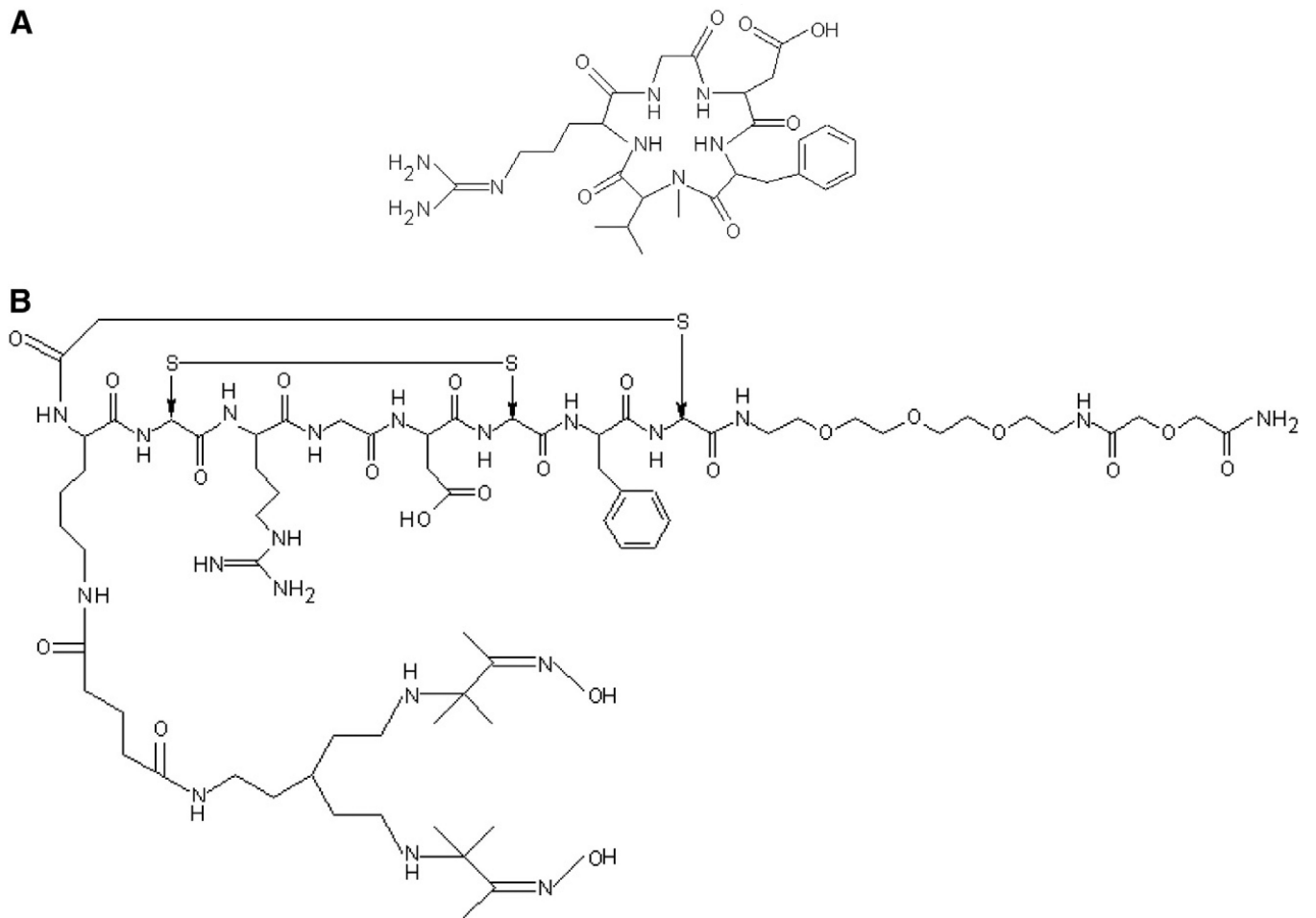
Acknowledgments

We thank Patricia Dunning, Erin Snay, Deviney Chaponis, Amanda Baker and Emily Greene for technical assistance. The assistance of Sharon Peled, PhD, in the acquisition of the MRI studies is gratefully acknowledged. Alice Carmel, BS, assisted with the mouse microSPECT studies. Kristin Johnson assisted with image preparation. NC100692 (maraciclalide) was provided by GE Health-care (Amersham, UK). EMD121974 (cilengitide) was provided by Merck KGaA (Darmstadt, Germany). This work was supported by the Childhood Brain Tumor Foundation, the Kyle Johnson Brain Tumor Fund, the CJ Buckley Brain Tumor Research Fund, the Stop&Shop Pediatric Brain Tumor Research Fund and the Ralph and Andrea Faber Fund for Radiological Research. The microSPECT camera was purchased with NIH Grant S10-RR17224.

References

1. Alghisi GC, Ruegg C. Vascular integrins in tumor angiogenesis: mediators and therapeutic targets. *Endothelium*. 2006; 13:113–135. [PubMed: 16728329]
2. Brooks PC, Clark RA, Cheresch DA. Requirement of vascular integrin alpha v beta 3 for angiogenesis. *Science*. 1994; 264:569–571. [PubMed: 7512751]
3. Haubner R, Wester HJ, Reuning U, Senekowitsch-Schmidtke R, Diefenbach B, Kessler H, et al. Radiolabeled alpha(v)beta3 integrin antagonists: a new class of tracers for tumor targeting. *J Nucl Med*. 1999; 40:1061–1071. [PubMed: 10452325]
4. Beer AJ, Schwaiger M. Imaging of integrin alphavbeta3 expression. *Cancer Metastasis Rev*. 2008; 27:631–644. [PubMed: 18523730]
5. Dumont RA, Deininger F, Haubner R, Maecke HR, Weber WA, Fani M. Novel (64)Cu- and (68)Ga-labeled RGD conjugates show improved PET imaging of alpha(nu) beta(3) integrin expression and facile radiosynthesis. *J Nucl Med*. 2011; 52:1276–1284. [PubMed: 21764795]
6. Hua J, Dobrucki LW, Sadeghi MM, Zhang J, Bourke BN, Cavaliere P, et al. Noninvasive imaging of angiogenesis with a ^{99m}Tc -labeled peptide targeted at alphavbeta3 integrin after murine hindlimb ischemia. *Circulation*. 2005; 111:3255–3260. [PubMed: 15956134]
7. Dobrucki LW, Tsutsumi Y, Kalinowski L, Dean J, Gavin M, Sen S, et al. Analysis of angiogenesis induced by local IGF-1 expression after myocardial infarction using microSPECT-CT imaging. *J Mol Cell Cardiol*. 2010; 48:1071–1079. [PubMed: 19850049]
8. Bach-Gansmo T, Danielsson R, Saracco A, Wilczek B, Bogsrud TV, Fangberget A, et al. Integrin receptor imaging of breast cancer: a proof-of-concept study to evaluate ^{99m}Tc -NC100692. *J Nucl Med*. 2006; 47:1434–1439. [PubMed: 16954550]
9. Bach-Gansmo T, Bogsrud TV, Skretting A. Integrin scintimammography using a dedicated breast imaging, solid-state gamma-camera and (^{99m}Tc -labelled NC100692. *Clin Physiol Funct Imaging*. 2008; 28:235–239. [PubMed: 18384623]
10. Axelsson R, Bach-Gansmo T, Castell-Conesa J, McParland BJ. An open-label, multicenter, phase 2a study to assess the feasibility of imaging metastases in late-stage cancer patients with the alpha

- v beta 3-selective angiogenesis imaging agent ^{99m}Tc -NC100692. *Acta Radiol.* 2010; 51:40–46. [PubMed: 20001475]
11. Indrevoll B, Kindberg GM, Solbakken M, Bjurgert E, Johansen JH, Karlsen H, et al. NC-100717: a versatile RGD peptide scaffold for angiogenesis imaging. *Bioorg Med Chem Lett.* 2006; 16:6190–6193. [PubMed: 17000103]
 12. Bruning A, Runnebaum IB. CAR is a cell-cell adhesion protein in human cancer cells and is expressionally modulated by dexamethasone, TNFalpha, and TGFbeta. *Gene Ther.* 2003; 10:198–205. [PubMed: 12571626]
 13. Moore, SC.; Mellen, R.; Lim, C-B. Modification of a triple-detector SPECT system for small-animal imaging. *IEEE Nucl. Sci. Symp. & Med. Imag. Conf.*; Portland, OR. 2003.
 14. Moore SC, Mahmood A, Mellen R, Lim C-B. A triple-detector, multiple-pinhole system for SPECT imaging of rodents. *J Nucl Med.* 2004; 45:97P.
 15. Chauvenet, W. A manual of spherical and practical astronomy V.II. Dover, NY: 1891. p. 474-566.
 16. Liu Z, Jia B, Shi J, Jin X, Zhao H, Li F, et al. Tumor uptake of the RGD dimeric probe (^{99m}Tc -G(3)-2P(4)-RGD2 is correlated with integrin alpha(v)beta(3) expressed on both tumor cells and neovasculature. *Bioconjug Chem.* 2010; 21:548–555. [PubMed: 20184307]
 17. Liu S, Hsieh WY, Jiang Y, Kim YS, Sreerama SG, Chen X, et al. Evaluation of a (^{99m}Tc) Tc-labeled cyclic RGD tetramer for noninvasive imaging integrin alpha(v)beta3-positive breast cancer. *Bioconjug Chem.* 2007; 18:438–446. [PubMed: 17341108]
 18. Wu Y, Zhang X, Xiong Z, Cheng Z, Fisher DR, Liu S, et al. microPET imaging of glioma integrin {alpha}v{beta}3 expression using (^{64}Cu)-labeled tetrameric RGD peptide. *J Nucl Med.* 2005; 46:1707–1718. [PubMed: 16204722]
 19. Kunstler JU, Seidel G, Bergmann R, Gniazdowska E, Walther M, Schiller E, et al. Novel ^{99m}Tc '4 + 1' peptide conjugates: tuning the biodistribution by variation of coligands. *Eur J Med Chem.* 2010; 45:3645–3655. [PubMed: 20570022]
 20. Decristoforo C, Santos I, Pietzsch HJ, Kuenstler JU, Duatti A, Smith CJ, et al. Comparison of in vitro and in vivo properties of [^{99m}Tc]cRGD peptides labeled using different novel Tc-cores. *Q J Nucl Med Mol Imaging.* 2007; 51:33–41. [PubMed: 17372571]
 21. Liu S, Hsieh WY, Kim YS, Mohammed SI. Effect of coligands on biodistribution characteristics of ternary ligand ^{99m}Tc complexes of a HYNIC-conjugated cyclic RGDfK dimer. *Bioconjug Chem.* 2005; 16:1580–1588. [PubMed: 16287258]



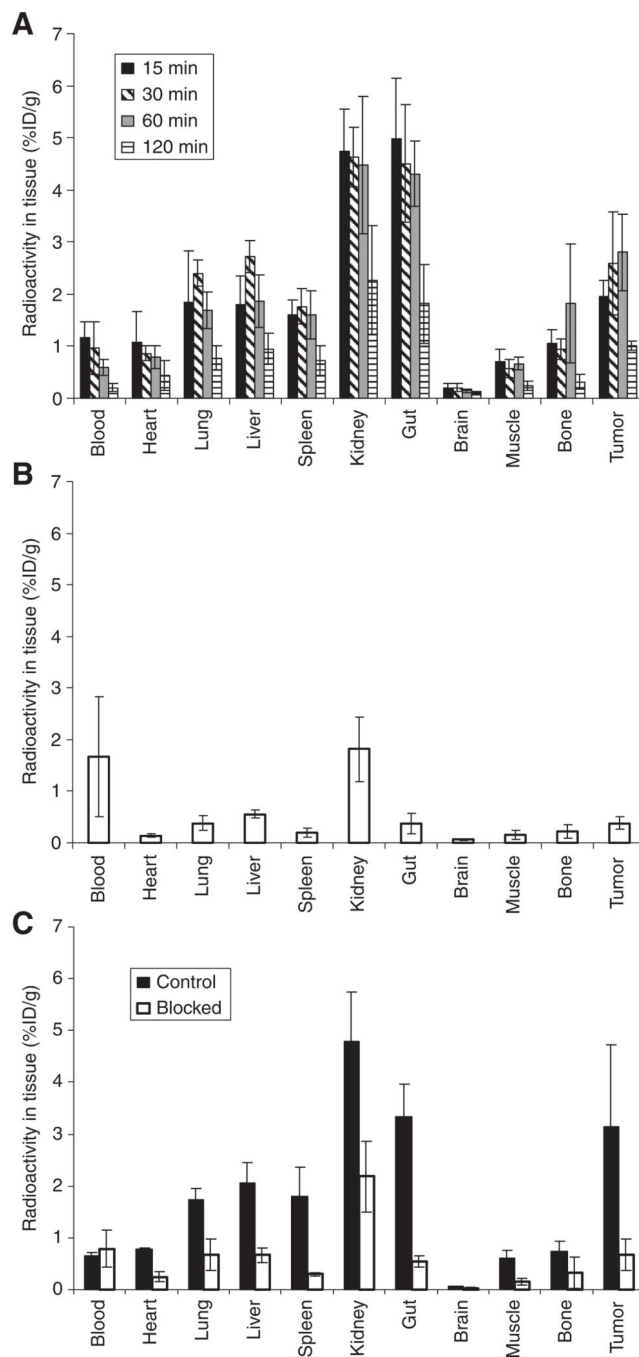


Fig. 2. Biodistribution data. (A) Tissue distribution of ^{99m}Tc -NC100692 in mice bearing subcutaneous U87MG tumors (percent injected dose per gram, %ID/g; $n = 5/6$). Tumor uptake peaked at around 30–60 min. (B) Biodistribution of ^{99m}Tc -labeled non-specific structural analogue of NC100692 at 60 min post-injection ($n = 5$). (C) Effect of blocking uptake with excess mass of NC100692; biodistribution at 30 min post-injection of ^{99m}Tc -NC100692 preceded by saline control (filled bars), and preceded by 2000-fold mass of

unlabeled NC100692 (unfilled bars) ($n = 4/5$). The same y-axes are used for ease of comparison.

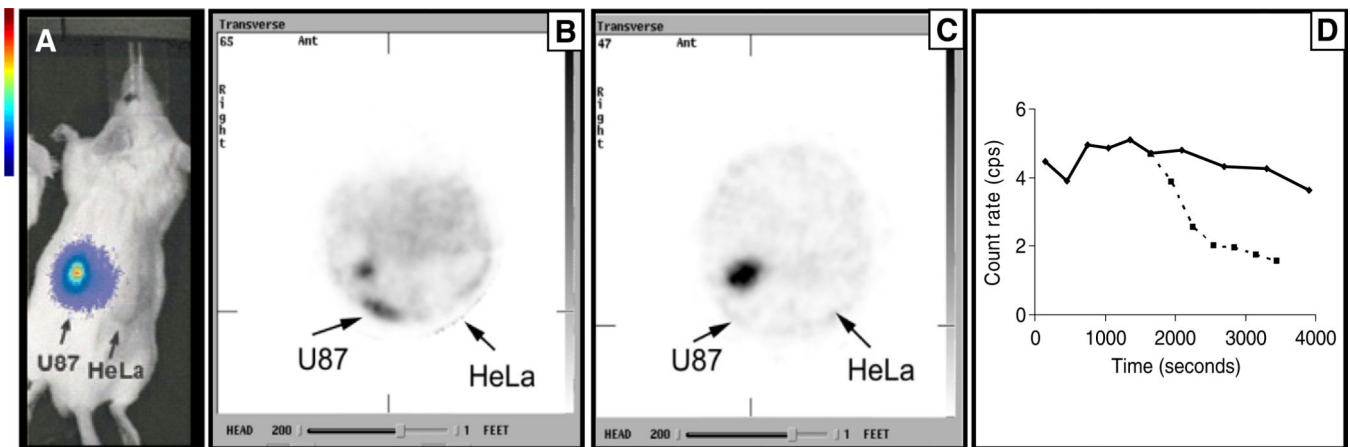


Fig. 3. MicroSPECT imaging of uptake of ^{99m}Tc -100692 by target-positive U87MG (bioluminescent image [A], color scale bar to the left) and target-negative HeLa subcutaneous tumors. (B) A transaxial slice through the microSPECT image with higher uptake in the U87MG (note high uptake in kidney). (C) The effect of i.p. injection of 50 mg/kg cilengitide 30 min after ^{99m}Tc -100692 injection. (D) The time-activity (counts per second; cps) curve for the uptake and washout of ^{99m}Tc -100692 in the U87MG tumor (solid line) and the displacement effect of cilengitide (dashed line). Mice were injected with 1 mCi of ^{99m}Tc , anesthetized using isoflurane (4% for induction, 1%–2% for maintenance) in oxygen, and imaged for 1 h.

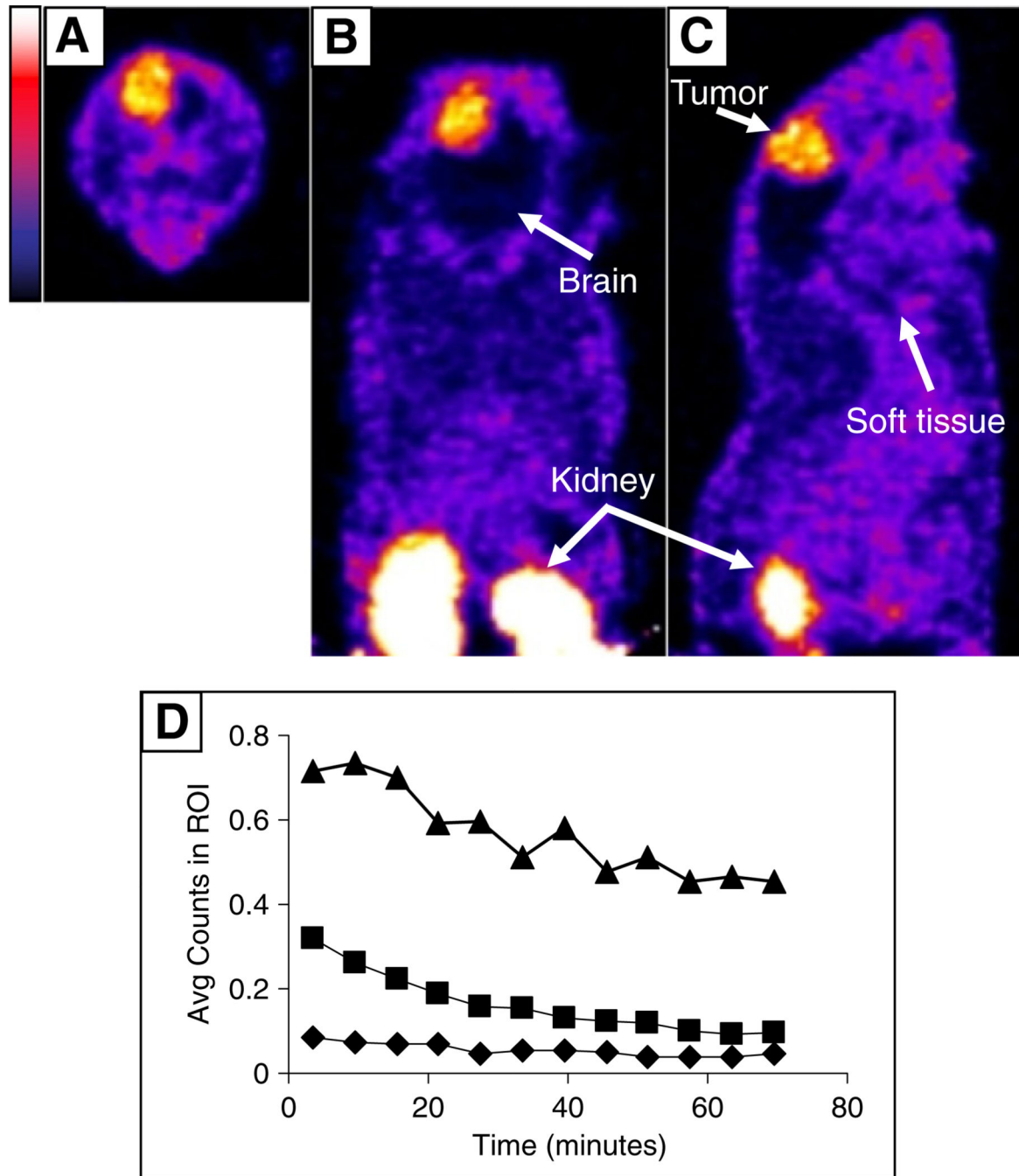


Fig. 4. Uptake of ^{99m}Tc -NC100692 in an intracerebral U87MG tumor. Transaxial (A), coronal (B) and sagittal (C) microSPECT images of the distribution of ^{99m}Tc -NC100692 in an orthotopic tumor are shown (color scale bar to the left). (D) The average data from regions of interest (ROI) drawn over the tumor (triangles), soft tissue (squares) and non-tumor brain (diamonds). Mice were injected with 1 mCi of ^{99m}Tc , anesthetized using isoflurane (4% for induction, 1%–2% for maintenance) in oxygen, and imaged for 1 h.

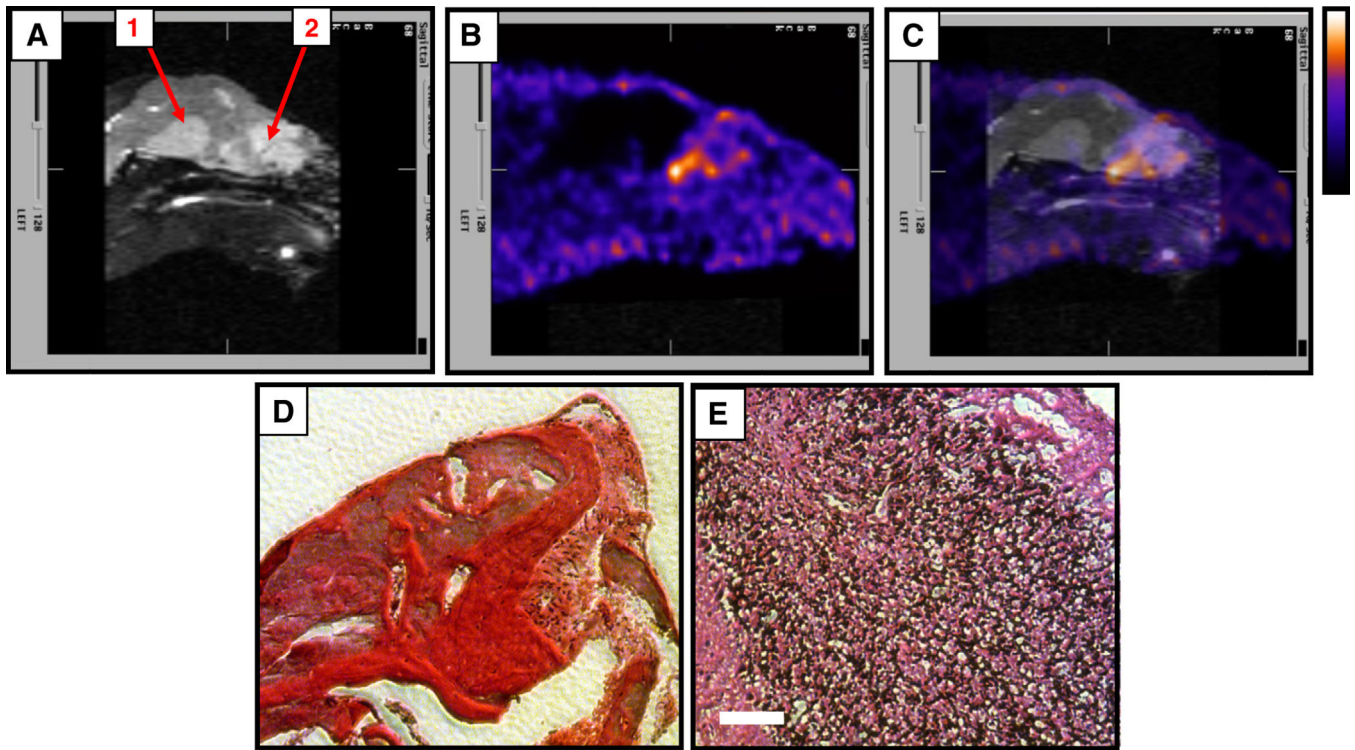


Fig. 5. Detection of orthotopic glioma. MRI (contrast enhanced, T_1 weighted) revealed two anomalies in the brain (A, regions 1 and 2), but only one was positive for ^{99m}Tc -NC100692 uptake (B, region 2; C, merged MR and microSPECT images, color scale bar to the right). Post-mortem histological analysis revealed that region 1 was hemorrhage (D), and that region 2 was a U87MG tumor lesion (E). Sections were stained using hematoxylin and eosin, and scale bar (white, E) is 100 μm . Mice were injected with 1 mCi of ^{99m}Tc , anesthetized using isoflurane (4% for induction, 1%–2% for maintenance) in oxygen, and imaged for 1 h.